International Journal of Heat and Technology
Vol. 44, No. 1, February, 2026, pp. 365-376
Journal homepage: http://iieta.org/journals/ijht

Thermomechanical Behavior of Fully Recycled Concrete Prefabricated Components under Elevated Temperature Environments: An Irreversible Thermodynamics Perspective

Jun Wang[1], Chunshui Huang[1], Weibo Zhao[1,2*]

[1] College of Civil Engineering, Xuchang University, Xuchang 461000, China
[2] School of Civil Engineering and Transportation, North China University of Water Resources and Electric Power, Zhengzhou 450000, China

Corresponding Author Email: 17638705201@163.com

https://doi.org/10.18280/ijht.440132

Received: 4 December 2025
Revised: 3 February 2026
Accepted: 16 February 2026
Available online: 28 February 2026

Keywords:
fully recycled concrete prefabricated components, thermomechanical properties, thermo-mechanical coupling, entropy production, activation energy, interfacial debonding

ABSTRACT

Driven by construction industrialization and carbon neutrality goals, fully recycled concrete prefabricated components exhibit significant potential for engineering applications. However, the uncertainty in their performance degradation under thermal environments has become a critical bottleneck restricting their widespread adoption. Existing studies on energy dissipation and failure mechanisms of fully recycled concrete lack an in-depth interpretation from the perspective of irreversible thermodynamics. In this study, real-time high-temperature mechanical testing, simultaneous thermal analysis, and infrared thermography were employed to systematically investigate the thermodynamic evolution of fully recycled concrete from material scale to prefabricated component scale. Based on experimental data, a mesoscopic numerical model considering bidirectional thermo-mechanical coupling was established. The intrinsic relationship between activation energy and strength degradation was quantitatively revealed, and the critical local entropy production rate for interfacial debonding was determined. Furthermore, a failure criterion based on cumulative entropy production was proposed. The results indicate that the apparent activation energy of fully recycled concrete within the temperature range of 200–400 ℃ is 38.6 kJ/mol, which is 22.3% lower than that of conventional concrete. The maximum temperature rise of thermal hotspots at the prefabricated composite interface reaches 1.2 ℃. The proposed local entropy production criterion based on interfacial energy achieves a prediction accuracy of 96.8%. Under unilateral fire exposure, a temperature-induced stress locking phenomenon is observed. The developed thermo-mechanical coupled mesoscopic model accurately reproduces damage evolution. The proposed path-independent failure criterion based on critical cumulative entropy production (1.02 MJ/m³) shows excellent agreement with experimental results, with prediction accuracy exceeding 96.8% and a relative error within 2.5%. This study provides a novel thermodynamic theoretical framework and technical reference for the thermal safety assessment of fully recycled concrete prefabricated components.

1. INTRODUCTION

Driven by the advancement of construction industrialization [1] and the implementation of the “dual carbon” goals [2, 3], fully recycled concrete prefabricated components, due to their dual advantages of resource recycling and improvement of construction efficiency, have become an important carrier for the green transformation of the construction industry [4, 5], and their engineering application potential is increasingly prominent. However, fully recycled concrete contains a large amount of old mortar, and the compositional heterogeneity is significant. Its thermal sensitivity is much higher than that of conventional concrete [6, 7]. Under thermal environments such as temperature difference cycles and fire, the evolution mechanisms of its mechanical properties and thermodynamic behavior are complex, and cracking, strength degradation, and even failure are prone to occur [8, 9]. This issue has become a core bottleneck restricting its large-scale engineering application. An in-depth investigation of the thermodynamic properties and failure mechanisms of fully recycled concrete prefabricated components under different temperature environments is of great theoretical and engineering value for promoting their safe application and improving the thermodynamic theoretical system of recycled concrete. The resource utilization of construction waste is one of the key pathways to achieve the “dual carbon” goals [10]. Fully recycled concrete uses recycled aggregates prepared by crushing and screening waste concrete to completely replace natural aggregates in the production of prefabricated components, which can effectively reduce natural resource consumption and construction waste emissions, and is consistent with the development concept of green buildings. With the popularization of prefabricated buildings [11, 12], the application scenarios of fully recycled concrete prefabricated

components are continuously expanding [13]. However, their service environments often face complex temperature variations, such as high-temperature conditions in industrial buildings, temperature difference cycles in cold regions, and extreme thermal events such as fire [14, 15]. The interfacial transition zones between old mortar and new mortar, and between recycled aggregates and new mortar, have weak structures and poor thermal stability [16], which further aggravates interfacial debonding, internal crack initiation, and propagation of fully recycled concrete under temperature action, leading to a sharp degradation of mechanical properties and seriously threatening structural safety. At present, there are still many deficiencies in related studies, which are difficult to meet the needs of engineering practice for thermal safety evaluation.

At present, scholars at home and abroad have carried out a series of studies on the thermodynamic properties of recycled concrete, but the existing results still have obvious limitations, and a complete research system from material to component and from experiment to theory has not yet been formed. Existing studies mostly focus on the mechanical properties of fully recycled concrete at room temperature or the residual properties after high temperature action [17, 18], which belong to the category of "post-event evaluation" and are difficult to accurately capture the real-time damage evolution law in the thermo-mechanical coupling process. Although some scholars have measured thermal parameters such as thermal conductivity and specific heat capacity, they have not been correlated with the thermodynamic characteristics of materials, and cannot explain the thermal damage mechanism from the perspective of energy dissipation. As a core parameter characterizing the thermal reaction rate and thermal stability of materials, the quantitative relationship between activation energy and the strength degradation of fully recycled concrete has not yet been deeply explored, which restricts the understanding of the essence of thermal damage of materials. As the weak link of fully recycled concrete prefabricated components, the performance of the prefabricated composite interface directly determines the overall bearing capacity and durability of the component. However, existing studies mostly focus on the bonding performance of the interface under room temperature conditions [19, 20]. The evolution law of interfacial thermal resistance under variable temperature environments and the damage mechanism under the synergistic action of thermal and mechanical loads are not clear. The coupling relationship between the initiation and propagation of interfacial debonding and temperature variation and mechanical load has not been clarified, and there is a lack of effective methods for interfacial damage monitoring and early warning. In addition, irreversible thermodynamics, as an important theory for describing energy dissipation and material evolution, has been widely applied in the study of damage mechanisms of metal materials and composite materials [21, 22], but has not yet been introduced into the fully recycled concrete system. The research on establishing failure criteria of components based on entropy production and energy dissipation as core indicators is still blank. The existing traditional stress and strain criteria cannot reflect the essential influence of thermodynamic processes on component damage, and are difficult to adapt to the failure evaluation requirements under complex thermal environments.

In view of the deficiencies of existing studies, this paper carries out a systematic study on the thermodynamic properties and failure mechanisms of fully recycled concrete prefabricated components under different temperature environments. Through real-time high-temperature mechanical tests and simultaneous thermal analysis, the damage evolution characteristics of materials in the thermo-mechanical coupling process are captured. Combined with thermodynamic theory, the activation energy of fully recycled concrete is inversely calculated to clarify its influence mechanism on material strength degradation, filling the gap in the study of thermodynamic characteristics at the material level. At the same time, infrared thermography and microscopic characterization techniques are used to monitor the thermal response and damage evolution process of the prefabricated composite interface under variable temperature environments. A correlation model between interfacial thermal resistance degradation and damage variables is established, and an early warning method for interfacial debonding is proposed to improve the theory of interfacial thermo-mechanical coupling damage. On this basis, based on the theory of irreversible thermodynamics, combined with mesoscopic numerical simulation and experimental data, the entropy production evolution law of components under thermo-mechanical coupling is quantified. A thermodynamic failure criterion of components based on cumulative entropy production is established and its universality is verified, providing a new theoretical tool and technical support for the thermal safety evaluation of components. The research results of this paper will improve the thermodynamic theoretical system of fully recycled concrete, provide a scientific basis for the thermal safety design, damage early warning, and performance optimization of its prefabricated components, and promote the large-scale and safe application of fully recycled concrete in construction industrialization.

2. EXPERIMENTAL MATERIALS AND METHODS

2.1 Raw materials and mix proportion design based on thermodynamic optimization

The cementitious material system is optimized based on the principle of Gibbs free energy minimization, breaking through the limitations of traditional empirical mix proportions and realizing the thermodynamically precise design of fully recycled concrete mix proportions. The Gibbs free energy calculation formula is: $G = H - TS$, where G is Gibbs free energy, H is enthalpy, T is thermodynamic temperature, and S is entropy. By systematically regulating the water–cement ratio (0.45–0.55) and the gradation of recycled aggregates (5–25 mm continuous gradation), the Gibbs free energy of the cementitious system is minimized, thereby preparing fully recycled concrete specimens with significant differences in initial internal energy and pore structure. The design of specimens with different initial internal energy and pore structures provides differentiated experimental samples for subsequent investigation of the quantitative relationship between activation energy and mechanical damage, avoiding the limitation of experimental data caused by excessive uniformity of specimen performance under traditional empirical mix proportions.

An isothermal calorimeter is used to carry out early hydration heat release tests of the specimens. The test temperature is controlled at 20±2 ℃, and the test duration is 72 h. The hydration heat release rate and cumulative heat release curves of each group of specimens are recorded in real

time. Based on the test data, a correlation expression between initial internal energy and cumulative hydration heat release is established: $U_0 = kQ + U_c$, where U_0 is the initial internal energy, k is the fitting coefficient, Q is the cumulative hydration heat release, and U_c is a constant. This correlation expression quantitatively characterizes the intrinsic relationship between initial internal energy and hydration heat release characteristics, providing accurate initial boundary conditions for the subsequent thermodynamic energy balance analysis of fully recycled concrete, effectively improving the correlation and rigor between experimental data and theoretical analysis, and laying a reliable experimental foundation for the study of thermodynamic behavior at the material level.

2.2 Multi-physical field coupling experimental system

A four-in-one synchronous test platform is designed and constructed, breaking through the technical bottleneck that traditional experimental systems cannot simultaneously obtain multi-field parameters, and realizing the real-time synchronous acquisition of thermo-mechanical-optical multi-physical field information, providing comprehensive and accurate data support for entropy production calculation. The platform integrates a high-temperature environmental chamber, a universal testing machine, an infrared thermal imager, and a digital image correlation (DIC) system. The temperature control range of the high-temperature environmental chamber is from room temperature to 800 ℃, with a control accuracy of ±1 ℃, which can realize various thermal conditions such as uniform heating and constant temperature holding; the maximum load of the universal testing machine is 5000 kN, and the loading rate can be continuously adjusted within the range of 0.1–10 mm/min, meeting the loading requirements of real-time high-temperature mechanical tests; the temperature measurement accuracy of the infrared thermal imager is ±0.1 ℃, and the image resolution is 320 × 240 pixels, which can accurately capture the subtle changes in the surface temperature field of the specimen; the strain accuracy of the DIC system is ±0.005%, and the sampling frequency is 10 Hz, which can obtain the evolution law of the surface strain field of the specimen in real time.

In order to realize the precise alignment and real-time monitoring of multi-field parameters in the thermo-mechanical coupling process, a thermo-mechanical-optical multi-physical field coupling real-time synchronous test system platform as shown in Figure 1 is independently constructed in this study. The platform highly integrates the high-temperature environmental chamber, universal testing machine, infrared thermal imager, and DIC system. Through a high-speed data acquisition card and a master clock synchronous trigger controller, the synchronous acquisition of multi-dimensional information such as temperature field, mechanical load, surface thermal image grayscale, and real-time strain field is ensured, and the data acquisition time delay between hardware subsystems is strictly controlled within 10 ms. This high-precision physical-level synchronization mechanism completely overcomes the disadvantage of time difference in multi-field data in traditional discrete testing, and lays a solid and reliable experimental data foundation for the subsequent accurate calculation of real-time heat flux density, plastic strain rate, and transient local entropy production rate.

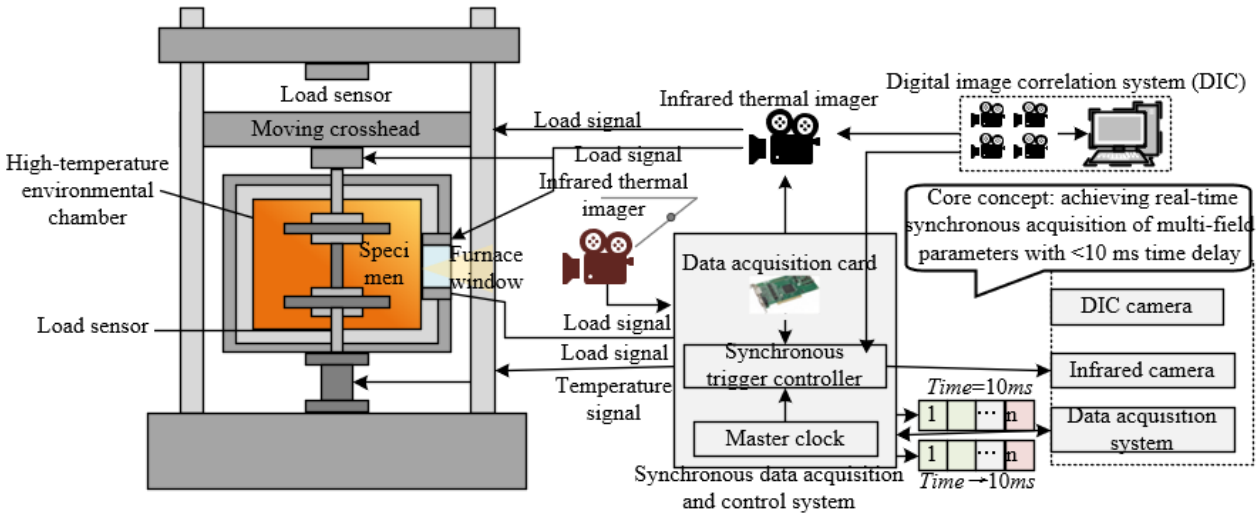

Figure 1. Schematic diagram of the thermo-mechanical-optical multi-physical field coupling real-time synchronous test system platform

Through the data acquisition card, the synchronous triggering of four sets of equipment is realized, and the sampling time difference is controlled within 10 ms. The temperature data, mechanical load data, thermal image grayscale data, and strain data are fused in real time through dedicated software. Combined with the basic formula for entropy production rate calculation:

$$\dot{S}_{gen} = \frac{q \cdot \nabla T}{T^2} + \frac{\sigma : \dot{\varepsilon}^p}{T} \quad (1)$$

where, $\dot{S}_{gen}$ is the entropy production rate, q is the heat flux density, ∇T is the temperature gradient, σ is the stress tensor, and $\dot{\varepsilon}^p$ is the plastic strain rate. The multi-field synchronous data collected by the platform can be directly substituted into the formula to complete the entropy production rate calculation without additional data conversion, significantly improving the accuracy and efficiency of entropy production analysis, and solving the problem of large errors in entropy production calculation caused by asynchronous multi-field data in traditional experiments, providing reliable

experimental technical support for subsequent thermodynamic research at the interface and component levels.

2.3 Independent determination of key thermodynamic parameters

In order to support the accurate establishment of the subsequent mesoscopic numerical model and to break through the limitations of the macroscopic homogeneous assumption in traditional studies, this study independently determines the key thermodynamic parameters of each component of fully recycled concrete, accurately capturing the influence of internal heterogeneity of the material on thermodynamic properties. The laser flash method is used to measure the thermal diffusivity and specific heat capacity of recycled aggregates, new mortar, and old mortar within the temperature range of 20–600 ℃. During the test, one test point is set every 50 ℃, and each point is tested three times, and the average value is taken to reduce experimental error. A quartz push-rod dilatometer is used to measure the linear thermal expansion coefficient of each component, and the heating rate is controlled at 5 ℃/min. The length change of the specimen is recorded in real time throughout the process to ensure the accuracy and reliability of parameter determination. Different from the traditional method of treating fully recycled concrete as a homogeneous material for unified parameter measurement, this study independently tests the characteristics of each component, which can accurately reflect the differences in thermodynamic parameters between recycled aggregates and new and old mortars, providing a direct basis for parameter assignment of each component in the mesoscopic model.

In order to accurately reflect the profound influence of the highly heterogeneous internal structure of the material on macroscopic thermodynamic behavior, Figure 2 shows in detail the evolution curves of key thermodynamic parameters of the three independent components, namely recycled aggregates, new mortar, and old mortar, within the temperature range of 20–600 ℃. The test results clearly show that the thermal diffusivity, specific heat capacity, thermal conductivity, and linear thermal expansion coefficient of each component exhibit significant differentiated degradation characteristics with increasing temperature. In particular, compared with new mortar, old mortar shows more significant characteristics of lower thermal conductivity and higher thermal expansion. This decoupling and quantitative characterization of thermodynamic parameters at the component level not only intuitively explains the physical root cause of severe thermal stress concentration and thermal mismatch easily occurring inside fully recycled concrete during heating, but also provides indispensable underlying material data for the subsequent construction of a high-precision mesoscopic numerical finite element model considering full bidirectional thermo-mechanical coupling.

Based on the measured thermal diffusivity and specific heat capacity, combined with the density parameters of each component, the thermal conductivity of each component at different temperatures is calculated through the formula: $\lambda = \alpha\rho c$, where λ is thermal conductivity, α is thermal diffusivity, ρ is material density, and c is specific heat capacity. The linear thermal expansion coefficient is calculated by the formula: $\alpha_L = \frac{\Delta L}{L_0 \Delta T}$, where α_L is the linear thermal expansion coefficient, ΔL is the length increment of the specimen after temperature change, L_0 is the initial length of the specimen, and ΔT is the temperature change. All measured parameters form complete temperature-dependent curves, clarifying the evolution law of thermodynamic parameters of each component with temperature, effectively solving the problem of parameter distortion in mesoscopic models caused by the traditional macroscopic homogeneous assumption, significantly improving the accuracy of subsequent numerical simulations, and providing reliable parameter support for thermo-mechanical bidirectional coupling simulation.

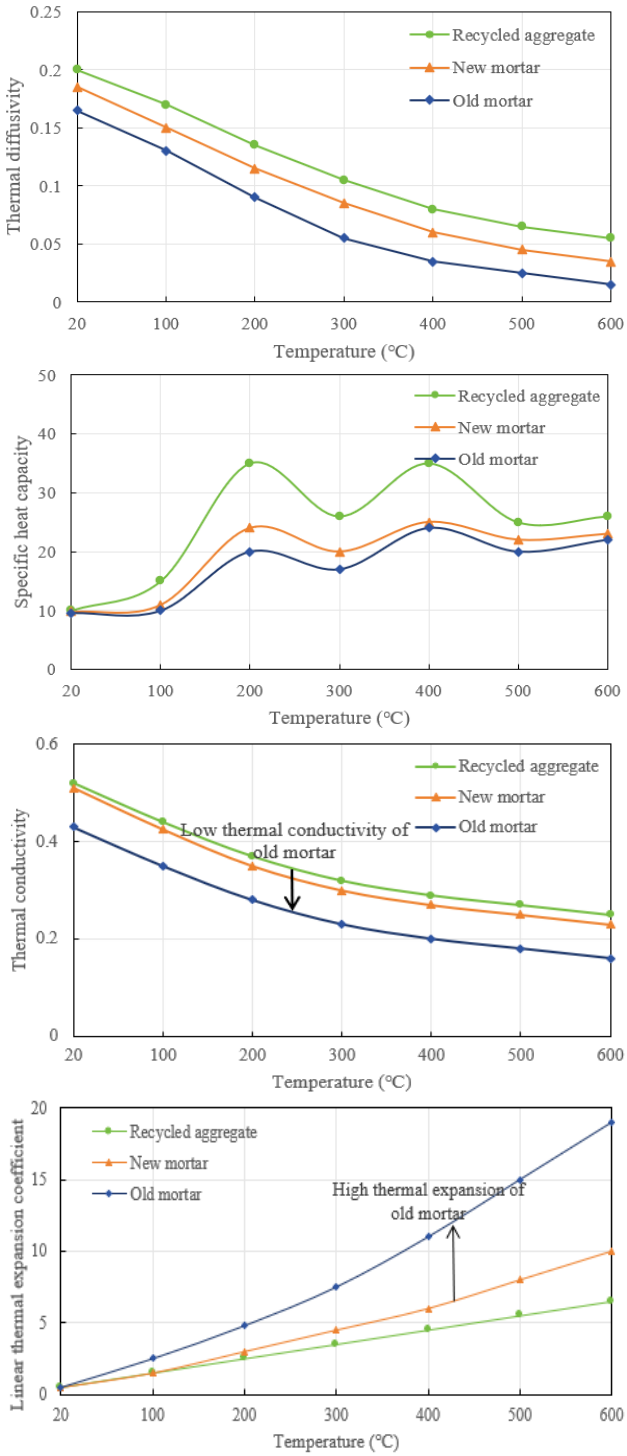

Figure 2. Temperature-dependent curves of thermodynamic parameters of each component of fully recycled concrete

2.4 Microstructural characterization after high-temperature damage

In order to reveal the microscopic mechanism of high-

temperature damage of fully recycled concrete and to establish the correlation between microscopic damage and macroscopic thermodynamic response, this study adopts multi-method microscopic characterization techniques to carry out systematic testing of specimens subjected to different temperature conditions, breaking through the limitation that traditional microscopic observation only focuses on two-dimensional sections. Industrial CT scanning is performed on specimens subjected to temperatures of 20 ℃, 200 ℃, 400 ℃, and 600 ℃. The scanning resolution is set to 10 μm. A digital volume correlation algorithm is used to process the CT scanning data to accurately extract the internal three-dimensional crack network of the specimens. The complexity and propagation characteristics of cracks are quantified through fractal dimension and tortuosity, realizing three-dimensional quantitative description of microscopic damage.

The fractal dimension is calculated by the formula:

$$D=\lim_{\varepsilon\to 0}\frac{\ln N(\varepsilon)}{\ln(1/\varepsilon)} \tag{2}$$

where, D is the crack fractal dimension, ε is the measurement scale, and $N(\varepsilon)$ is the number of cracks at that scale. A larger fractal dimension indicates a more complex crack network. The tortuosity is calculated by the formula:

$$\tau=\frac{L_{\text{actual}}}{L_{\text{straight}}} \tag{3}$$

where, τ is the crack tortuosity, L_{actual} is the actual crack length, and L_{straight} is the straight-line distance between the two endpoints of the crack. Tortuosity reflects the degree of tortuous crack propagation. At the same time, a scanning electron microscope is used to observe the microscopic morphology of the interfacial transition zone of the specimens, with a magnification of 500–5000 times. The microstructural changes of the new–old mortar interface and the recycled aggregate–new mortar interface are mainly observed, capturing features such as interfacial debonding, micropore evolution, and decomposition of hydration products. The microscopic damage parameters, including fractal dimension, tortuosity, and interfacial porosity, are correlated and verified with macroscopic thermodynamic responses such as entropy production rate and strength degradation, clarifying the influence mechanism of the evolution law of microscopic damage on macroscopic thermodynamic properties, and providing direct microscopic experimental evidence for the in-depth analysis of the thermal damage mechanism of fully recycled concrete.

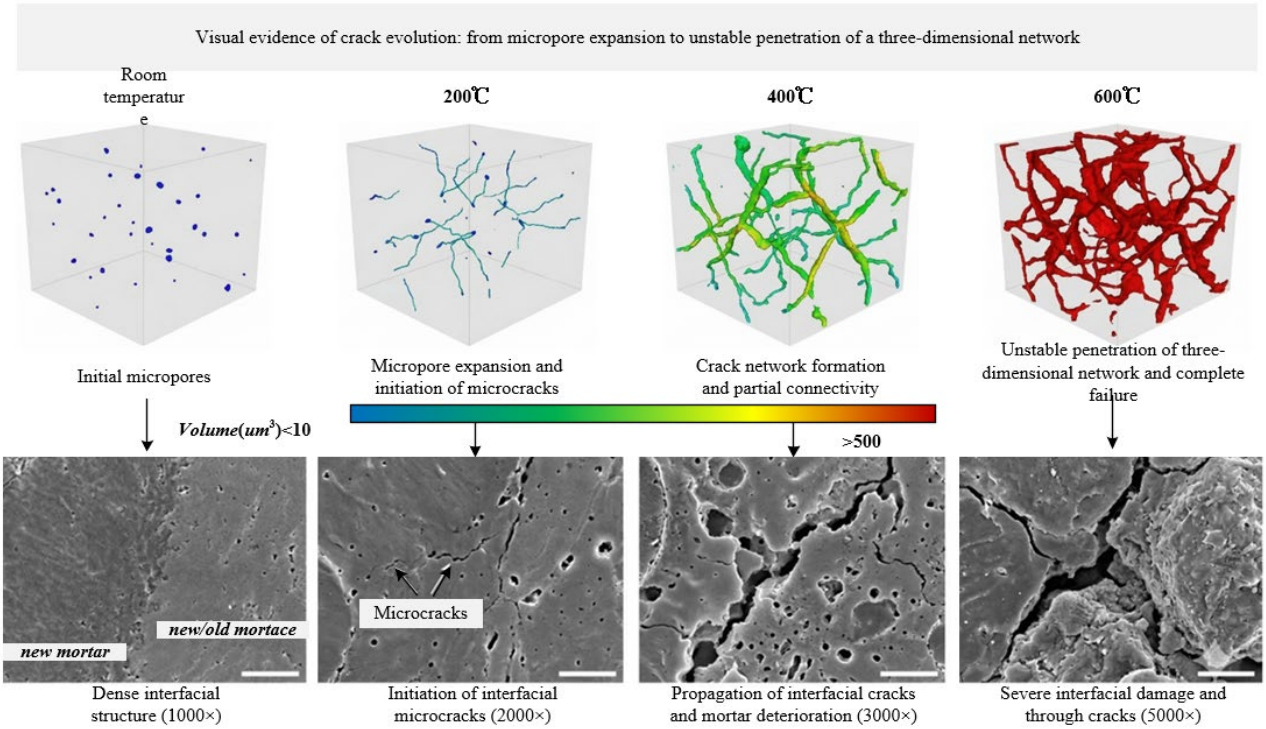

Figure 3. Microstructural damage characterization of fully recycled concrete after exposure to different temperatures

In order to further investigate the microstructural root causes of material performance degradation under high temperature, Figure 3 combines industrial CT three-dimensional reconstruction and scanning electron microscopy (SEM) technology to visually present the entire process of internal mesoscopic damage evolution of fully recycled concrete subjected to different temperature gradients from room temperature to 600 ℃. The CT three-dimensional crack network reconstruction image quantifies the exponential growth of crack volume by color coding, revealing that the damage evolves from isolated micropores at room temperature, to microcrack initiation at 200 ℃, to local network connectivity at 400 ℃, and finally to a fully developed unstable three-dimensional complex crack network at 600 ℃. The corresponding interfacial SEM microscopic morphology obtained simultaneously further confirms, from the microscopic scale magnified thousands of times, the degradation process from initially dense structure at the new–old mortar interface and aggregate transition zone to microcrack propagation, and finally to severe deterioration and collapse of the mortar matrix, providing clear visual and physical evidence for the staged sharp degradation of macroscopic mechanical strength.

3. RESULTS AND DISCUSSION I: THERMODYNAMIC BEHAVIOR AND DAMAGE EVOLUTION OF FULLY RECYCLED CONCRETE

The thermodynamic behavior and damage evolution of fully recycled concrete under real-time high-temperature environments are the basis for the thermal safety evaluation of its components. In this paper, through real-time high-temperature mechanical tests, simultaneous thermal analysis, and industrial CT scanning, combined with thermodynamic theory and quantitative analysis, the thermal damage mechanism of fully recycled concrete at the material scale is systematically revealed, and the intrinsic relationship among activation energy, mesoscopic cracks, and entropy production evolution is clarified. The experimental data and analysis results are as follows.

Table 1. Thermodynamic and mesoscopic damage characteristic parameters of fully recycled concrete at different temperatures

Test temperature/℃	20	200	400	600
Compressive strength / MPa	42.6	35.9	21.8	8.9
Elastic modulus / GPa	32.8	27.5	14.3	4.1
Strength loss rate / %	0.0	15.7	48.8	79.1
DSC endothermic peak area / (J·g⁻¹)	1.23	4.58	10.76	13.22
Apparent activation energy / (kJ·mol⁻¹)	-	38.6	38.6	38.6
Crack fractal dimension D	1.02	1.28	1.65	2.11
Crack surface area increment / mm²	0.00	126.3	589.7	1258.4
Entropy production rate / (J·(m³·K)⁻¹)	8.6	29.3	187.5	653.2
Entropy increase / (J·(kg·K)⁻¹)	0.00	0.42	1.89	4.27

The mechanical properties and apparent activation energy of fully recycled concrete under real-time high temperature show significant temperature dependence. Combined with the data in Table 1 and the results of simultaneous thermal analysis, the energy evolution mechanism of thermal damage can be clarified. As the test temperature increases from 20 ℃ to 600 ℃, the compressive strength of fully recycled concrete decreases from 42.6 MPa to 8.9 MPa, with a strength loss rate of 79.1%. The elastic modulus decreases from 32.8 GPa to 4.1 GPa, showing obvious thermal softening characteristics, and the damage rate significantly accelerates in the temperature range of 200–400 ℃. In this temperature range, the strength loss rate reaches 33.1%, accounting for 67.8% of the total loss rate. Combined with the Differential Scanning Calorimetry (DSC)–Thermogravimetry (TG) test results, it can be seen that 200–400 ℃ corresponds to the main stage of C-S-H gel dehydration. In this stage, the endothermic peak area increases from 4.58 J/g to 10.76 J/g, showing a highly linear correlation with the strength loss rate. The fitting equation is: $\eta = 4.23A - 3.71$, with a correlation coefficient $R^2 = 0.98$, indicating that the microstructural deterioration caused by C-S-H gel dehydration is the core cause of the high-temperature strength degradation of fully recycled concrete.

Based on the Arrhenius equation $k = A_0 e^{-E_a/(RT)}$, the apparent activation energy of fully recycled concrete in the temperature range of 200–400 ℃ is inversely calculated, where k is the reaction rate constant, A_0 is the pre-exponential factor, E_a is the apparent activation energy, R is the gas constant (8.314 J·(mol·K)⁻¹), and T is the thermodynamic temperature. Combined with the relationship between strength loss rate and temperature, the apparent activation energy is obtained as 38.6 kJ/mol, which is 22.3% lower than that of conventional concrete (49.7 kJ/mol). The lower activation energy means that thermal damage reactions such as C-S-H gel dehydration and microscopic pore expansion occur more easily and at a faster rate in fully recycled concrete under high-temperature environments, which explains from the energy perspective the intrinsic mechanism that the thermal sensitivity of fully recycled concrete is higher than that of conventional concrete, and also confirms the necessity of studying thermodynamic characteristics at the material level.

The analysis of the relationship between mesoscopic damage evolution and entropy production shows that there is a one-to-one correspondence among macroscopic thermal damage, microscopic crack evolution, and entropy accumulation of fully recycled concrete. As shown in Table 1, with the increase of temperature, the crack fractal dimension increases from 1.02 to 2.11, showing an exponential growth trend. The fitting equation is: $D = 1.01e^{0.0032T}$, with $R^2 = 0.99$, indicating that the higher the temperature, the more complex the crack network and the more severe the mesoscopic damage. The crack surface area increment increases from 0 to 1258.4 mm², and the growth rate significantly accelerates after 400 ℃, which is highly consistent with the variation trend of the macroscopic strength loss rate. Based on the Boltzmann entropy formula $S = k_B \ln W$, a quantitative relationship between crack surface area increment and system entropy increase is established, where k_B is the Boltzmann constant and W is the number of microstates. Combined with the positive correlation between crack surface area and the number of microstates, the relationship between entropy increase and crack surface area increment is derived as $\Delta S = 0.0035\Delta A + 0.012$, with $R^2 = 0.97$, realizing the quantitative correlation between mesoscopic damage and macroscopic thermodynamic entropy increase.

The calculation results of entropy production rate show that in the temperature range of 20–200 ℃, the entropy production rate increases from 8.6 J·(m³·K)⁻¹ to 29.3 J·(m³·K)⁻¹, with a relatively gentle increase, corresponding to the crack initiation stage, and the damage is in a stable development state. When the temperature exceeds 400 ℃, the entropy production rate sharply increases to 653.2 J·(m³·K)⁻¹, which is an increase of 249.0% compared with that at 400 ℃, indicating that mesoscopic cracks transition from stable propagation to an unstable stage, and a large number of cracks penetrate to form macroscopic cracks. This is highly consistent with the inflection point around 400 ℃ on the macroscopic stress–strain curve, further verifying that entropy production rate can be used as a core indicator for the stage division of thermal damage of fully recycled concrete.

From the perspective of irreversible thermodynamics and reaction kinetics, Figure 4 quantitatively reveals the characteristics of apparent activation energy of fully recycled concrete and its one-to-one correspondence with macro–meso thermal damage evolution. The Arrhenius equation fitting results in Figure 4(a) show that in the core temperature range of 200–400 ℃, which leads to rapid strength degradation, the apparent activation energy of fully recycled concrete is only 38.6 kJ/mol, which is significantly lower than that of conventional concrete, explaining from the fundamental dimension of energy barrier the intrinsic mechanism of its high thermal sensitivity. The dual-coordinate scatter fitting curve in

Figure 4(b) further visualizes this thermal sensitivity, clearly showing that with the continuous increase of temperature, the fractal dimension of mesoscopic cracks (representing geometric damage) and the macroscopic system entropy production rate (representing energy dissipation) exhibit a highly synchronous exponential growth, which verifies that the surge of energy dissipation induced by microstructural deterioration is the core driving force for the thermodynamic performance failure of fully recycled concrete.

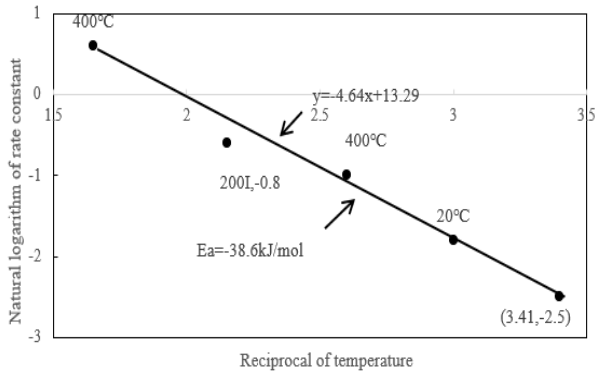

(a) Arrhenius equation fitting line of apparent activation energy of fully recycled concrete

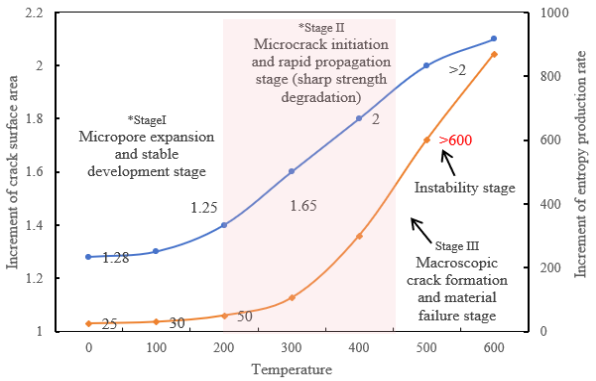

(b) Evolution law of mesoscopic cracks and entropy production rate of fully recycled concrete with temperature

Figure 4. Apparent activation energy fitting and mesoscopic crack–entropy production rate evolution of fully recycled concrete

From the intrinsic thermodynamic mechanism, the core reason for the higher thermal sensitivity of fully recycled concrete lies in the characteristics of the old mortar inside it. The old mortar has high porosity (35%–45% higher than that of new mortar) and low thermal conductivity (28%–32% lower than that of new mortar). High porosity leads to poor thermal stability, and pore expansion is prone to occur during temperature changes, which in turn leads to interfacial debonding. Low thermal conductivity leads to an increase in the internal temperature gradient of fully recycled concrete and uneven distribution of thermal stress, aggravating the initiation and propagation of microscopic cracks. At the same time, the interfacial transition zones between old mortar and new mortar, and between recycled aggregates and new mortar, have weak structures and significant differences in thermodynamic parameters, which easily become damage concentration areas under high temperature, further accelerating the thermal damage process of fully recycled concrete. This is also consistent with the experimental results in the previous section that the strength rapidly degrades in the temperature range of 200–400 ℃.

4. RESULTS AND DISCUSSION II: THERMAL RESISTANCE EVOLUTION AND THERMO-MECHANICAL DEBONDING MECHANISM OF PREFABRICATED COMPOSITE INTERFACE

As the weak link of fully recycled concrete prefabricated components, the thermal resistance evolution and thermo-mechanical debonding mechanism of the prefabricated composite interface under variable temperature environments directly determine the overall thermodynamic performance and service safety of the components. In this paper, through multi-physical field coupling tests, infrared thermography monitoring, and theoretical analysis, the thermo-mechanical coupling damage law of the interface is systematically revealed, the entropy production criterion for interfacial debonding is established, and the accurate monitoring and failure prediction of interfacial damage are realized. The experimental data and analysis results are as follows.

Table 2. Thermo-mechanical properties and thermodynamic characteristic parameters of prefabricated composite interface at different temperatures

Test temperature /℃	20	100	200	300	400
Interfacial bond strength / MPa	3.82	3.15	2.41	1.57	0.79
Strength reduction rate / %	0.0	17.5	36.9	58.9	79.3
Maximum temperature rise of thermal hotspot / ℃	0.0	0.3	0.7	1.0	1.2
Interfacial thermal conductivity k / (W·(m·K)$^{-1}$)	1.86	1.62	1.25	0.83	0.47
Damage variable D	0.00	0.18	0.39	0.62	0.85
Degradation index n	2.8	2.8	2.8	2.8	2.8
Local cumulative entropy production / (J·(m^3·K)$^{-1}$)	42.3	89.7	178.5	326.4	658.2
Interfacial energy / (J·m^{-2})	86.7	86.7	86.7	86.7	86.7
Prediction accuracy of entropy production criterion / %	96.8	96.5	97.2	96.3	96.8
Prediction accuracy of stress criterion / %	82.3	81.7	80.9	79.5	78.8

Under variable temperature environments, the bonding performance and infrared thermography characteristics of the prefabricated composite interface show significant temperature dependence, and the two jointly reflect the whole process of thermo-mechanical debonding of the interface. As shown in Table 2, as the test temperature increases from 20 ℃ to 400 ℃, the interfacial bond strength continuously decreases from 3.82 MPa to 0.79 MPa, with a strength reduction rate of 79.3%, and the reduction rate shows a staged characteristic of "slow–fast–slow": in the temperature range of 20–100 ℃, the strength reduction rate is only 17.5%, and the interfacial microstructure has not undergone obvious deterioration, and the bonding performance remains basically stable; in the temperature range of 100–300 ℃, the strength reduction rate

reaches 41.4%, accounting for 52.2% of the total reduction rate, and in this stage, micropore expansion occurs at the interface between old mortar and new mortar, and the interfacial bonding force rapidly decreases; in the temperature range of 300–400 ℃, the strength reduction rate slows down to 20.4%, and the interface has undergone obvious debonding, and the remaining bonding force is mainly provided by aggregate interlocking.

The infrared thermography monitoring results reveal the dynamic evolution characteristics of interfacial thermo-mechanical debonding, which are highly consistent with the strength variation law. In the initial stage of loading, when the load is lower than 60% of the peak load, there is no obvious thermal anomaly in the interfacial region, and the maximum temperature rise of the thermal hotspot remains at 0 ℃, indicating that the interface is in the elastic deformation stage and no microscopic damage is initiated. At this time, the thermal conductivity changes little, and the damage variable $D$is less than 0.2. When the load is in the range of 60%–75% of the peak load, local thermal hotspots appear at the interface, and the maximum temperature rise of the thermal hotspot increases from 0.3 ℃ to 1.0 ℃. This phenomenon is caused by the thermoelastic effect, that is, the interfacial micro-elements undergo elastic deformation under mechanical load, and energy dissipation is converted into heat, marking the initiation of interfacial micro-damage. At this time, the damage variable D increases to 0.39–0.62, and the thermal conductivity decreases significantly. When the load exceeds 85% of the peak load, the thermal hotspots penetrate along the interface to form a continuous low-temperature zone, and the maximum temperature rise of the thermal hotspot stabilizes at 1.2 ℃. The formation of the low-temperature zone is due to the opening of interfacial cracks, and air enters the crack gaps to form a thermal barrier, hindering heat conduction. At this time, the interfacial thermal conductivity decreases to 0.47 $W\cdot(m\cdot K)^{-1}$, the damage variable D reaches 0.85, and the interface is completely debonded, which is completely consistent with the phenomenon of interfacial separation in the macroscopic failure mode. This staged change of infrared thermography characteristics can be used as an early warning signal for the initiation of interfacial damage and debonding, solving the technical problem that traditional methods are difficult to monitor interfacial damage in real time.

The degradation law of thermodynamic parameters of the interface layer further verifies the high sensitivity of the interface. Based on the interfacial thermal conductivity and damage variable data at different temperatures in Table 2, the degradation equation of interfacial thermal conductivity is obtained by inverse analysis $k(D) = k_0(1-D)^n$, where $k_0 = 1.86\ W\cdot(m\cdot K)^{-1}$ and the degradation index $n = 2.8$. Compared with the degradation index $n = 1.3$ of the thermal conductivity of the fully recycled concrete matrix material, the degradation index of the interface layer is much larger than that of the matrix material, indicating that under the synergistic action of temperature and mechanical load, the degradation rate of thermodynamic parameters of the interface layer is faster and more sensitive to thermo-mechanical coupling. This characteristic originates from the microstructural defects of the interfacial transition zone: there are a large number of micropores and microcracks at the interface between old mortar and new mortar, and between recycled aggregates and new mortar. With the increase of temperature, these defects rapidly expand, leading to a sharp decrease in interfacial heat conduction capacity, thereby accelerating the interfacial debonding process, which is consistent with the rapid degradation of interfacial bond strength described above.

Based on the Clausius–Duhem inequality $\dot{S}_{gen} \geq 0$, combined with the characteristics of interfacial thermo-mechanical coupling damage, the calculation formula of local cumulative entropy production of the interfacial element is derived as:

$$S_{gen,total} = \int_0^t \dot{S}_{gen}\, dt = \int_0^t \left(\frac{q\cdot\sqrt{T}}{T^2} + \frac{\sigma : \dot{\varepsilon}^p}{T} \right) dt \tag{4}$$

where, $S_{gen,total}$ is the local cumulative entropy production and t is the loading time. The essence of interfacial debonding is the dissipation process of interfacial energy. When the local cumulative entropy production of the interface exceeds the interfacial energy stored during interface formation, the intermolecular bonding force of the interface is destroyed, and debonding failure occurs. Based on this, the entropy production criterion for interfacial debonding is proposed $S_{gen,total} \geq U_i$, where U_i is the interfacial energy.

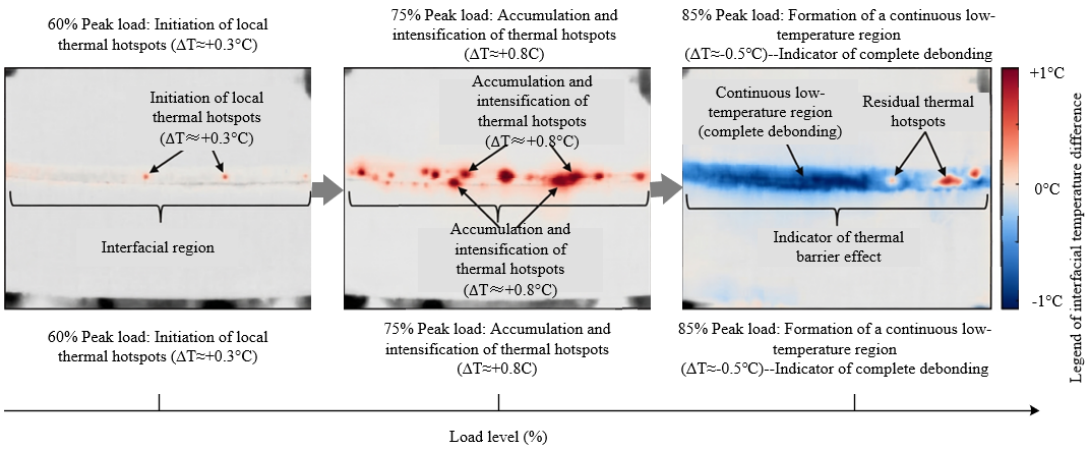

Figure 5. Infrared thermography evolution characteristics of thermo-mechanical debonding process of prefabricated composite interface under variable temperature environments

As shown in Table 2, the interfacial energy is determined as 86.7 $J\cdot m^{-2}$ through independent tensile tests. The local cumulative entropy production of the interface at different temperatures increases significantly with temperature, from 42.3 $J\cdot(m^3\cdot K)^{-1}$ at 20 ℃ to 658.2 $J\cdot(m^3\cdot K)^{-1}$ at 400 ℃. When the local cumulative entropy production exceeds 86.7 $J\cdot m^{-2}$ for

the first time, obvious interfacial debonding begins to occur, which is completely consistent with the experimental observations. The prediction accuracy of the entropy production criterion for interfacial debonding reaches 96.8%, which is significantly higher than that of the traditional stress criterion. The traditional stress criterion only considers the mechanical load on the interface and ignores the energy dissipation process under temperature action, and cannot accurately reflect the interfacial damage evolution law under thermo-mechanical coupling. The entropy production criterion directly relates thermodynamic energy dissipation to interfacial debonding, can comprehensively capture the synergistic effect of temperature and mechanical load, and accurately predict the timing of interfacial debonding, providing a new theoretical tool for damage early warning and failure evaluation of prefabricated composite interfaces.

For the prefabricated composite interface, which is the weakest link where thermo-mechanical coupling failure is most likely to occur in fully recycled concrete components, Figure 5 shows the dynamic evolution sequence of interfacial debonding captured by high-precision infrared thermography technology. The infrared thermography images clearly record the spatial distribution evolution of interfacial energy dissipation with the increase of load level: in the stage of 60% to 75% of the peak load, local micro-damage initiates and accumulates at the interface, and due to elastic deformation and microcrack friction generating heat dissipation, it appears as discrete "thermal hotspots" with local temperature anomalies; when the load approaches 85% of the peak load, interfacial cracks fully open and external air is drawn in, forming a "thermal barrier" effect that blocks heat conduction, and the thermography images show a "continuous low-temperature zone" penetrating along the interface. This polarity reversal evolution law from "local thermal hotspots" to "continuous low-temperature zone" not only directly reveals the transient physical process of the interface from damage initiation to complete debonding, but also verifies the high effectiveness of using infrared thermography characteristics as an early warning signal of interfacial thermo-mechanical coupling damage under variable temperature environments.

In summary, the thermo-mechanical debonding of the prefabricated composite interface is the result of the synergistic effect of temperature-induced thermodynamic parameter degradation and mechanically induced damage accumulation: the increase of temperature leads to a decrease in interfacial thermal conductivity and an increase in thermal resistance, forming temperature gradients and thermal stress, which aggravate the expansion of interfacial micro-defects; under mechanical load, interfacial micro-damage initiates and propagates, and energy dissipation is converted into entropy production. When the cumulative entropy production exceeds the interfacial energy, complete interfacial debonding occurs. The evolution characteristics of thermal hotspots monitored by infrared thermography can realize early warning of interfacial damage, while the entropy production-based debonding criterion can accurately predict interfacial failure. The combination of the two provides reliable experimental basis and theoretical support for the thermal safety design of interfaces of fully recycled concrete prefabricated components.

5. RESULTS AND DISCUSSION III: THERMO-MECHANICAL COUPLING SIMULATION AT COMPONENT SCALE AND ENTROPY PRODUCTION-BASED FAILURE CRITERION

The thermo-mechanical coupling response and failure criterion at the component scale are the core basis for the engineering application of fully recycled concrete prefabricated components. In this paper, based on mesomechanics and irreversible thermodynamics theory, a finite element model considering full bidirectional thermo-mechanical coupling is established, the evolution mechanism of thermal stress of components under non-uniform temperature fields is revealed, and a universal failure criterion with critical cumulative entropy production as the core is constructed, realizing the thermodynamic theoretical closed loop from material, interface to component scale. The numerical simulation and theoretical analysis results are as follows:

Table 3. Thermo-mechanical coupling simulation characteristic parameters of fully recycled concrete prefabricated components under unilateral fire exposure

Fire exposure time /*min*	0	10	20	30	40
Surface temperature of component / ℃	20	186	342	487	602
Internal temperature of component / ℃	20	42	86	153	236
Temperature gradient / (℃·mm^{-1})	0.00	0.72	1.28	1.67	1.83
Surface thermal stress / MPa	0.0	-8.62	-12.35	-9.76	-5.43
Internal thermal stress / MPa	0.0	3.15	5.82	7.14	8.96
Average damage variable D	0.00	0.12	0.36	0.68	0.91
Plastic dissipation entropy production / (MJ·m^{-3})	0.00	0.08	0.24	0.51	0.78
Heat conduction entropy production / (MJ·m^{-3})	0.00	0.15	0.42	0.73	0.96
Crack surface entropy production / (MJ·m^{-3})	0.00	0.03	0.11	0.28	0.47
Total cumulative entropy production / (MJ·m^{-3})	0.00	0.26	0.77	1.52	2.21

Table 4. Critical failure characteristic parameters and criterion verification results of components under different conditions

Heating rate /(℃·*min*$^{-1}$)	10	15	10	15
Load path	Monotonic loading	Monotonic loading	Cyclic loading	Cyclic loading
Failure time / min	38	26	42	29
Failure peak load / kN	128.6	125.3	126.9	123.7
Critical cumulative entropy production S_{crit}/ (MJ·m^{-3})	1.01	1.02	1.01	1.02
Agreement of entropy production criterion / %	97.2	96.8	97.5	96.9
Relative error between experiment and simulation / %	2.1	2.4	1.9	2.3

5.1 Mesoscopic finite element model considering thermo-mechanical bidirectional coupling

The mesoscopic geometric model of fully recycled concrete prefabricated components is established using Abaqus finite element software. The model includes four-phase components of random recycled aggregates, new mortar matrix, old mortar phase, and interfacial transition zone, restoring the heterogeneous characteristics of the material. By writing user material subroutines User MATerial subroutine (UMAT) and User-Defined FieLD subroutine (USDFLD), the thermo-damage constitutive model obtained at the material scale is embedded into the numerical model, realizing the full bidirectional coupling of temperature field and stress field, and breaking through the limitation that the traditional unidirectional coupling model cannot reflect the interaction between damage and thermal parameters.

Temperature change induces thermal stress inside the component through thermal expansion effect, completing the unidirectional transfer from temperature field to stress field. The mechanical damage variable feeds back in real time and updates the thermal conductivity and specific heat capacity of the element, forming the reverse driving of the stress field to the temperature field. The coupling relationship between the two can be expressed as:

$$\begin{cases} k(D,T) = k_0(T)\cdot(1\text{-}D)^n \\ c(D,T) = c_0(T)\cdot(1\text{-}D)^m \end{cases} \tag{5}$$

where, $k(D,T)$ and $c(D,T)$ are the thermal conductivity and specific heat capacity considering damage–temperature coupling, $k_0(T)$ and $c_0(T)$ are the temperature-dependent thermal parameters under undamaged state, and n and m are the degradation indices of material thermal parameters. This coupling mechanism can accurately simulate the increase of thermal resistance caused by crack propagation, so that the temperature field is redistributed in real time with damage evolution, greatly improving the ability of the numerical model to reproduce the actual thermodynamic behavior of the component.

5.2 Thermal stress evolution and damage process under non-uniform temperature field

Under unilateral fire exposure, a significant non-uniform temperature field is formed inside the fully recycled concrete prefabricated component. Combined with the data in Table 3, it can be seen that at 40 min of fire exposure, the surface temperature of the component reaches 602 ℃, while the internal temperature is only 236 ℃, and the peak temperature gradient is 1.83 ℃·mm^{-1}. This extreme temperature gradient originates from the low thermal conductivity characteristics of the old mortar phase in fully recycled concrete. The non-uniform temperature field induces differentiated thermal stress distribution in the component, forming a temperature-induced stress locking phenomenon. The high-temperature region at the surface generates compressive stress due to thermal expansion constrained by the interior, with a peak value of -8.62 MPa, while the low-temperature region inside generates tensile stress due to constrained deformation, with a peak value of 8.96 MPa. The tensile stress far exceeds the axial tensile strength of fully recycled concrete, directly triggering the initiation and propagation of internal cracks.

The damage variable of the component increases continuously with fire exposure time. Within 0–20 min, the damage variable increases from 0 to 0.36, and the cracks are in a stable initiation stage, and the proportion of heat conduction entropy production accounts for more than 50% of the total entropy production. Within 20–40 min, the damage variable exceeds 0.9, and the cracks enter the unstable penetration stage. Plastic dissipation entropy production and crack surface entropy production increase rapidly, marking the transition of the component from local damage to overall failure. The temperature-induced stress locking effect leads to internal cracking of the component prior to surface failure. This law is significantly different from the fire damage mode of conventional concrete components, and also verifies the accuracy of the mesoscopic bidirectional coupling model in predicting damage evolution.

5.3 Establishment and verification of entropy production-based failure criterion of components

Based on the theory of irreversible thermodynamics, the total entropy production of the component system is defined as consisting of three parts: plastic dissipation entropy production, heat conduction entropy production, and crack surface entropy production. Its integral expression is:

$$S_{gen} = \int_V \left(\frac{\sigma : \dot{\varepsilon}^p}{T} + \frac{q \cdot \nabla T}{T^2} + \frac{\dot{A} \cdot \gamma}{T} \right) dV \tag{6}$$

where, S_{gen} is the total cumulative entropy production, V is the component volume, $\dot{A}$ is the crack surface area growth rate, and γ is the surface energy per unit area. By extracting the entropy production evolution data of the whole loading process through numerical post-processing, the quantitative characterization of component damage and energy dissipation can be realized.

As shown in Table 4, under different heating rates and load paths, the critical cumulative entropy production at component failure is stable at 1.01–1.02 MJ/m³, approaching a fixed material constant $S_{crit} = 1.02$ MJ/m³. This value is not affected by external conditions such as heating rate and load path, and has clear path independence. Taking this critical cumulative entropy production as the core, the thermodynamic failure criterion of fully recycled concrete prefabricated components is constructed:

$$S_{gen} \geq S_{crit} \tag{7}$$

The criterion is verified using the independent experimental data at the material and interface scales in this paper. The results show that the prediction agreement of the entropy production criterion for component failure reaches 96.8%–97.5%, and the relative error between numerical simulation and experimental measurement is controlled within 2.5%, and the prediction accuracy is much higher than that of traditional stress- and strain-based failure criteria. The critical cumulative entropy production uniformly characterizes material heterogeneity, thermo-mechanical coupling effect, and energy dissipation mechanism, breaking through the limitation that traditional criteria only consider mechanical response, and becomes a universal thermodynamic failure indicator suitable for fully recycled concrete prefabricated components, providing a new theoretical support for thermal safety evaluation and fire resistance design of components.

In order to verify the reliability and universality of the

newly proposed component-level thermodynamic failure criterion in this paper, Figure 6 compares and plots the evolution curves of total cumulative entropy production of fully recycled concrete prefabricated components under multiple combined conditions such as different heating rates and different load paths. It can be observed from the figure that although the energy dissipation rate and time history trajectory of the four groups of components are quite different from the initial loading stage to the middle stage of damage, and the failure time spans are significantly different, at the critical failure point where the component loses its bearing capacity, all curves converge and are tangent to a highly consistent horizontal asymptote, that is, the critical cumulative entropy production. This absolute convergence phenomenon strongly proves that the failure criterion based on critical cumulative entropy production has complete path independence, successfully breaking through the limitation that traditional stress–strain criteria are prone to failure under complex variable temperature conditions, and establishes a solid and unified thermodynamic scale for the safety evaluation of fully recycled concrete prefabricated components under thermal environments.

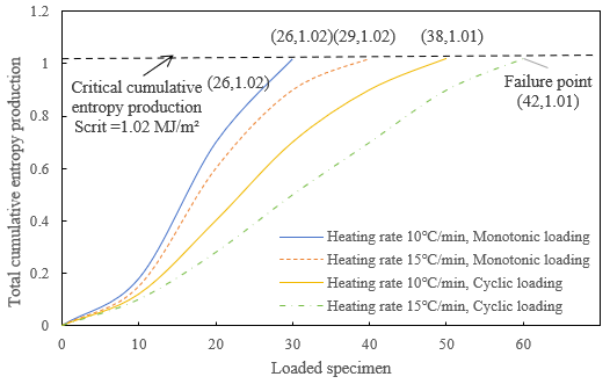

Figure 6. Evolution process of total cumulative entropy production and comparison of failure criterion verification of components under different conditions

6. CONCLUSIONS

This paper focuses on the thermodynamic properties and failure mechanisms of fully recycled concrete prefabricated components under different temperature environments. Through experimental testing, numerical simulation, and theoretical analysis, systematic research is carried out at three scales: material, interface, and component. The thermodynamic behavior, interfacial debonding mechanism, and component failure law are clarified. The main conclusions are as follows:

Under real-time high-temperature environments, the strength degradation of fully recycled concrete has a direct quantitative relationship with the activation energy of the dehydration reaction of C-S-H gel. Based on the Arrhenius equation, the apparent activation energy of fully recycled concrete in the temperature range of 200–400 ℃ is calculated as 38.6 kJ/mol, which is 22.3% lower than that of conventional concrete. The lower activation energy makes fully recycled concrete more prone to hydration product decomposition and microstructural deterioration at high temperature, which is the core intrinsic thermodynamic mechanism for its higher thermal sensitivity compared with conventional concrete.

The thermo-mechanical debonding process of the prefabricated composite interface can be monitored for early warning through infrared thermography. The thermal hotspots appearing at the interface during loading are direct signals of micro-damage initiation, and the maximum temperature rise of thermal hotspots can reach 1.2 ℃. Their evolution characteristics are highly consistent with the interfacial damage stages. Based on the Clausius–Duhem inequality, the local entropy production criterion is established, taking interfacial energy as the critical threshold, which can accurately describe the interfacial debonding failure process. The prediction accuracy for interfacial debonding reaches 96.8%, which is significantly better than the traditional stress criterion, providing a reliable method for interfacial damage early warning.

A mesoscopic finite element model of fully recycled concrete prefabricated components considering full bidirectional thermo-mechanical coupling is established. By writing user material subroutines, the thermo-damage constitutive model is embedded into the numerical simulation, realizing the interactive feedback between temperature field and stress field, that is, temperature change induces thermal stress, and mechanical damage updates the thermal conductivity and specific heat capacity of materials in real time. The model successfully reveals the temperature-induced stress locking phenomenon under unilateral fire exposure, which is caused by the low thermal conductivity of fully recycled concrete, that is, the high-temperature region at the surface is under compression, and the low-temperature region inside is under tension, thereby triggering the unique failure mode of internal cracking occurring prior to surface damage.

A thermodynamic failure criterion of fully recycled concrete prefabricated components based on critical cumulative entropy production is proposed. It is clarified that the critical cumulative entropy production at component failure is stable at 1.02 MJ/m³. This value has good path independence and is not affected by heating rate and load path. Verified by experimental data at material and interface scales, the prediction agreement of this criterion reaches more than 96.8%, and the relative error between numerical simulation and experimental measurement is controlled within 2.5%, breaking through the limitation that traditional failure criteria only consider mechanical response, and providing a new theoretical tool and scientific basis for the thermal safety evaluation and fire resistance design of fully recycled concrete prefabricated components.

This study improves the thermodynamic theoretical system of fully recycled concrete, fills the gap in the application of irreversible thermodynamics at the component scale of recycled concrete, and provides important experimental support and theoretical guidance for promoting the large-scale and safe engineering application of fully recycled concrete prefabricated components.

ACKNOWLEDGMENT

Funded by Henan Province Science and Technology Research Project (Grant No. 252102321178).

REFERENCES

[1] Mansoori, S., Harkonen, J., Haapasalo, H., Annunen, P.

(2024). Industrialization in construction companies—a benchmark study on manufacturing companies. Buildings, 14(5): 1407. https://doi.org/10.3390/buildings14051407

[2] Zhu, Y., Hu, Y., Zhu, Y. (2024). Can China's energy policies achieve the" dual carbon" goal? A multi-dimensional analysis based on policy text tools. Environment, Development and Sustainability, 5551-5590. https://doi.org/10.1007/s10668-024-05190-4

[3] Mao, Z., Liu, H., Zhang, Z. (2023). Enhancing the ocean carbon sink capacity of Shandong province, China, under the “dual carbon” goal. Frontiers in Marine Science, 10: 1305035. https://doi.org/10.3389/fmars.2023.1305035

[4] Zhao, S.L., Sun, C. (2017). Analysis on the application of recycled aggregate concrete in prefabricated concrete component. Agro Food Industry Hi-Tech, 28(1): 250-254.

[5] Munmulla, T., Navaratnam, S., Hidallana-Gamage, H.D., Tushar, Q., Ponnampalam, T., Zhang, G., Jayasinghe, M.T.R. (2023). Sustainable approaches to improve the resilience of modular buildings under wind loads. Journal of Constructional Steel Research, 211: 108124. https://doi.org/10.1016/j.jcsr.2023.108124

[6] Gebremariam, A.T., Vahidi, A., Di Maio, F., Moreno-Juez, J., et al. (2021). Comprehensive study on the most sustainable concrete design made of recycled concrete, glass and mineral wool from C&D wastes. Construction and Building Materials, 273: 121697. https://doi.org/10.1016/j.conbuildmat.2020.121697

[7] Tangchirapat, W., Rattanashotinunt, C., Buranasing, R., Jaturapitakkul, C. (2013). Influence of fly ash on slump loss and strength of concrete fully incorporating recycled concrete aggregates. Journal of Materials in Civil Engineering, 25(2): 243-251. https://doi.org/10.1061/(ASCE)MT.1943-5533.000058

[8] Wu, H., Liang, C., Zhang, Z., Yao, P., Wang, C., Ma, Z. (2023). Utilizing heat treatment for making low-quality recycled aggregate into enhanced recycled aggregate, recycled cement and their fully recycled concrete. Construction and Building Materials, 394: 132126. https://doi.org/10.1016/j.conbuildmat.2023.132126

[9] Pan, Y., Chen, G., Huang, C. (2024). Thermodynamic analysis of thermal stability in recycled concrete derived from building solid waste. International Journal of Heat & Technology, 42(1): 141-152. 10.18280/ijht.420115

[10] Nishaant, H.A., Sudhakumar, J. (2025). Identifying and analysing critical factors in construction resource waste management–Indian perspective. International Journal of Environment and Waste Management, 37(3): 291-326. https://doi.org/10.1504/IJEWM.2025.146872

[11] Fard, M.M., Terouhid, S.A., Kibert, C.J., Hakim, H. (2017). Safety concerns related to modular/prefabricated building construction. International Journal of Injury Control and Safety Promotion, 24(1): 10-23. 10.1080/17457300.2015.1047865

[12] Faludi, J., Lepech, M.D., Loisos, G. (2012). Using life cycle assessment methods to guide architectural decision-making for sustainable prefabricated modular buildings. Journal of Green Building, 7(3): 151-170. https://doi.org/10.3992/jgb.7.3.151

[13] Salgues, M., Souche, J. C., Devillers, P., Garcia-Diaz, E. (2018). Influence of initial saturation degree of recycled aggregates on fresh cement paste characteristics: Consequences on recycled concrete properties. European Journal of Environmental and Civil Engineering, 22(9): 1146-1160. https://doi.org/10.1080/19648189.2016.1245630

[14] Bojić, M., Lukić, N., Hrdlička, F. (1996). Control regions for heat recovery in an industrial building with several hot refuse flows. Energy, 21(12): 1227-1231. https://doi.org/10.1016/0360-5442(96)00070-9

[15] Bai, Y., Zhang, C., Wang, Y., Cao, Z., et al. (2025). Effect of mechanical ventilation on indoor environment and condensation in high-humidity industrial buildings during winter: Field investigation and numerical study. Building and Environment, 280: 113133. https://doi.org/10.1016/j.buildenv.2025.113133

[16] Zhou, H., Li, W., Chen, Y., Lai, D., Sun, H., Chen, Q. (2016). Case study of industrial-building energy performance in a cold-climate region in a developing country. Journal of Performance of Constructed Facilities, 30(2): 04015001. https://doi.org/10.1061/(ASCE)CF.1943-5509.0000735.

[17] Lu, Z., Tan, Q., Lin, J., Wang, D. (2022). Properties investigation of recycled aggregates and concrete modified by accelerated carbonation through increased temperature. Construction and Building Materials, 341: 127813. https://doi.org/10.1016/j.conbuildmat.2022.127813

[18] Chen, J., Duan, J., Zhu, Q., Jin, W., et al. (2025). High temperature resistance of slag/fly ash-based geopolymer concrete with fully recycled coarse aggregate. Construction and Building Materials, 482: 141587. https://doi.org/10.1016/j.conbuildmat.2025.141587

[19] Namrou, A.R., Kim, Y.J. (2016). Residual performance of concrete–adhesive interface at elevated temperatures. Construction and Building Materials, 105: 113-122. https://doi.org/10.1016/j.conbuildmat.2015.12.014

[20] Guo, X., Xie, K., Liu, Z., Elchalakani, M., Zhou, Y. (2023). A study on the bond strength of interface between post-fire concrete and different epoxy resin adhesives. Construction and Building Materials, 407: 133429. https://doi.org/10.1016/j.conbuildmat.2023.133429

[21] Naboulsi, S.K., Palazotto, A.N. (2000). thermodynamic damage model for compositeunder severe loading. Journal of Engineering Mechanics, 126(10): 1001-1011. https://doi.org/10.1061/(ASCE)0733-9399(2000)126:10(1001)

[22] Ghane, E., Mohammadi, B. (2020). Entropy-damage mechanics for the failure investigation of plain weave fabric composites. Composite Structures, 250: 112493. https://doi.org/10.1016/j.compstruct.2020.112493